EES Batteries

Check for updates

Approaching convergence in the electrochemical mechanism of aqueous Zn–MnO$_2$ sustainable batteries†

Balaji Sambandam, [ID] * Vinod Mathew, Muhammad H. Alfaruqi, Sungjin Kim and Jaekook Kim [ID] *

Manganese oxide cathodes are quite appealing when considering moderate energy/power aqueous rechargeable zinc-ion batteries (ARZIBs) and long-term cycling. However, due to the variety of potential reaction pathways that are periodically proposed, the electrochemistry of manganese oxides with zinc is still unclear and fraught with dispute. Several mechanisms have been hypothesized/proposed over time for Zn–MnO$_2$ in most common electrolyte of ZnSO$_4$, including exclusive Zn^{2+} insertion, exclusive H$^+$ conversion along with reversible layer hydroxide formation–dissolution, mixed insertion–conversion with and without layer formation–dissolution, exclusive MnO$_2$/Mn^{2+} electrodeposition–dissolution with layer formation–dissolution, and mixed electrodeposition–dissolution and Zn^{2+}/H$^+$ insertion with layer formation–dissolution. To tackle this problem, we propose three potential roadmap approaches: selection of operando analyses, fine-tuned electrolyte pH, and electrolyte isotope labelling.

Broader context

In developing efficient green-energy storage systems, the electrochemistry of manganese oxides for aqueous rechargeable zinc-ion batteries (Zn–MnO$_2$) is controversial due to numerous proposed reactions. A specific manganese oxide polymorph under similar electrochemical conditions shows distinct behavior in the common ZnSO$_4$ electrolyte, leading to misconceptions that hinder electrochemical performance and commercialization. While electrodeposition–dissolution is considered a major reaction, the ion intercalation mechanism should be verified in all polymorphs, except for δ-MnO$_2$, which has already been confirmed. However, the nature of the inserting ion remains unclear. To address all these issues, we suggest real-time analyses, including neutron diffraction and electron paramagnetic resonance spectroscopy, to investigate Zn^{2+}/H$^+$ intercalation and MnO$_2$/Mn^{2+} electrodeposition–dissolution reactions. Applying these techniques on a known MnO$_2$ polymorph with fine-pH-tuned electrolytes would help clarify the mechanism. Other operando and non-operando analyses should also be explored. Manganese dissolution is critical in Zn–MnO$_2$ batteries, and our initiation of AIMD simulations examines the manganese dissolution in detail.

1. Introduction

In the pursuit of renewable and clean energy to meet future demands, aqueous batteries have garnered increasing attention for their safety and potential as advanced technologies in the future.[1] Among aqueous energy storage technologies, aqueous Zn-metal-based batteries are particularly noteworthy because of their compatibility with water-based aqueous electrolytes and their high theoretical energy density (~820 mA h g^{-1} and ~5854 A h L^{-1}) as anodes. These include alkaline Zn–MnO$_2$ batteries, Zn–air batteries, mildly acidic aqueous

rechargeable Zn-ion batteries (ARZIBs), and electrolytic Zn–MnO$_2$ batteries with decoupled electrolytes.

Among these Zn-metal aqueous rechargeable batteries, ARZIBs and Zn–MnO$_2$ decoupled batteries, which have had a recent re-birth, are promising technologies aimed at greater utilization in stationary energy storage applications. The former has great potential due to high energy density, but there are many unaddressed factors, including the selection of a suitable membrane and cell design. On the other hand, ARZIBs typically operate in mildly acidic electrolytes with varied cathodes such as manganese oxides, making them a potential candidate for broadening suitable stationary energy storage systems (SESSs) through ease of cell assembling, high compatibility of the Zn anode in a mildly acidic medium (pH range 4–5) and environmental benignity.[2] Despite these advantages, the fundamental electrochemical mechanism associated with Zn–MnO$_2$ ARZIBs remains unaddressed, which impedes

Department of Materials Science and Engineering, Chonnam National University, Gwangju 61186, South Korea. E-mail: balajisam@chonnam.ac.kr, jaekook@chonnam.ac.kr

further developments.[3] Taking this opportunity, the benchmark roadmap strategies on the electrochemical mechanism of Zn–MnO$_2$ ARZIBs are provided here. This effort can remove the existing ambiguity related to the existing diverse theories and promote the realization of a unified conclusion on the electrochemical mechanism of ARZIBs.

2. Rapid emergence and controversial mechanism of mildly acidic aqueous Zn–MnO$_2$ batteries

AZIBs have been a highly researched topic since the conception of a mildly acidic Zn–MnO$_2$ battery with the ZnSO$_4$ electrolyte, which is the electrolyte used in the majority of cases in this field, with reversible Zn-ion intercalation in 2012. The increasingly voluminous research publications (Fig. S1 in the ESI†) and technology transfers reported so far testify to the fact that zinc hydroxide sulphate precipitation resulting from Zn^{2+} and/or H$^+$ insertion and Mn electrodissolution is a large contributor to the capacity and electrochemical results. This system is considered as a green, sustainable and renewable technology due to the low cost, safety, and environmental friendliness.[2,4] Specifically, the Zn–MnO$_2$ system with a considerably moderate voltage potential (∼1.3 V vs. Zn^{2+}/Zn) and sufficient energy storage capability (100–140 W h L^{-1}), reported from two start-ups,[5,6] shows commercial prospects for stationary energy storage system applications.

Despite these advantages, the dispute over the electrochemical reaction related to this aqueous electrolyte-based battery system with a MnO$_2$ cathode has persisted owing to the diverse mechanisms proposed by different research groups. Over the past decade, paradoxical electrochemical reactions on MnO$_2$, its polymorphs (α, β, δ, ε, and γ and a special structure), and related manganese oxides (MnO, Mn$_3$O$_4$, Mn$_2$O$_3$, and ZnMn$_2$O$_4$) have been continuously reported in ZnSO$_4$ electrolytes. These reactions include exclusive Zn^{2+} insertion, exclusive H$^+$ conversion, Zn^{2+}/H$^+$ co-insertion, mixed insertion–conversion, Zn^{2+}/H$^+$ insertion with Mn^{2+}/MnO$_2$ electrodissolution–deposition, Zn$_4$(OH)$_6$SO$_4$·nH$_2$O deposition/dissolution resulting from H$^+$ contribution, exclusive Mn^{2+}–MnO$_2$ electrodissolution–deposition, and exclusive H$^+$ insertion.[7] Specifically, manganese oxides have grossly different crystal structures and permit insertion of varying amounts of Zn^{2+}, H$^+$ and co-intercalated solvents upon electrochemical charge/discharge. Most recent studies suggested that Zn$_4$(OH)$_6$SO$_4$·nH$_2$O precipitation–decomposition resulting from H$^+$ (H$_3$O$^+$) and Mn^{2+}–MnO$_2$ electrodissolution–deposition is found to be major contributors to the capacity and resulting electrochemical mechanisms. However, all these manganese oxide-related cathode materials display almost identical galvanostatic discharge–charge profiles in the ZnSO$_4$ electrolyte with and without Mn^{2+} additives, except the initial cycles, thus making the analysis of the reaction mechanism more complex than anticipated.[8] Furthermore, the presence of Mn^{2+} additives, commonly MnSO$_4$, in electrolytes also intensifies matters, leading to increased complexity to assess the mechanism. A few of the recent reports have mainly centered on settling the electrochemical mechanism debate by calling for convergence towards a unified electrochemical theory for Zn–MnO$_2$ batteries.[8,9] These reports conclude that the debate between Zn^{2+} and H$^+$ (co-) intercalation mechanisms and the MnO$_2$–Mn^{2+} electrodeposition–dissolution mechanism for Zn–MnO$_2$ ARZIBs remains a close-call, needing urgent resolution via deeply investigating operando-assisted techniques.

For example, two separate studies, in recent times, presented conflicting findings regarding the impact of H$^+$ intercalation on MnO$_2$ cathodes.[2,9] One study demonstrated its exclusive contribution, while the other indicated just a minimal contribution from H$^+$ towards energy storage. In contrast, a very recent mechanism proposed involves Zn^{2+}/H$^+$ co-intercalation, accompanied by Mn^{2+} electrodissolution, in a MnO$_2$ polymorph, as illustrated in Fig. 1, through various electrochemical analyses including oper-

Balaji Sambandam is a Research Professor at the department of Materials science and Engineering, Chonnam National University, South Korea. He completed his B.Sc/M.Sc and Ph.D. in chemistry, respectively, from Bharathidasan University and Anna University, Tamil Nadu, India. He received Institute Post-doctoral fellowship from Indian Institute of Technology-Madras. His research interests include designing electrode materials for energy applications, especially Zn batteries.

Balaji Sambandam

Sungjin Kim is a Research Professor at the Department of Materials science and Engineering, Chonnam National University (CNU), South Korea. He received B.S., M.S., and Ph.D. from CNU. His research focuses on design and development of electrode materials for non-aqueous Li/Na-ion and aqueous Zn batteries energy applications.
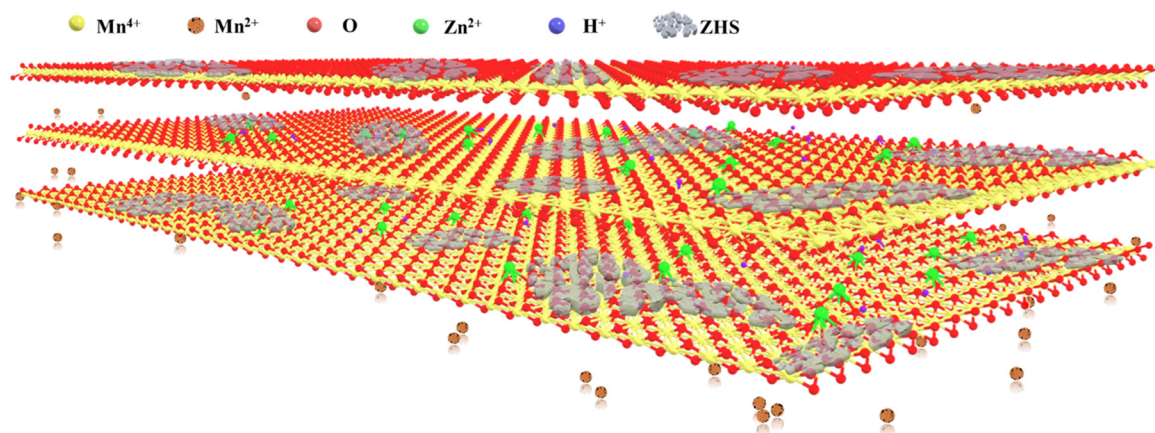
Sungjin Kim

Fig. 1 With conflicting electrochemical reaction mechanisms in aqueous Zn–MnO$_2$ batteries, possible proposed storage mechanisms include Mn electrodissolution–deposition, H$^+$ and/or Zn^{2+} intercalation–deintercalation and ZHS (Zn$_4$(OH)$_6$SO$_4$·nH$_2$O) deposition–dissolution are depicted in δ-MnO$_2$, a layered phase, from a pool of available MnO$_2$ polymorphs.

ando and non-operando techniques. Notably, most of the reported MnO$_2$ polymorphs and their related oxides do not provide solid evidence of Zn^{2+}/H$^+$ co-intercalation *via* operando X-ray diffraction analysis (XRD) probably due to their distinct crystal structures.[7] This has led to a few groups dismissing intercalation feasibility and suggesting that the sole action of MnO$_2$–Mn^{2+} electrodeposition–dissolution drives the capacity contribution in Zn–MnO$_2$ batteries.[8] These ongoing debates suggest that resolving the mechanism debate (listed in Table 1 in the ESI†) is intricate and remains fully unaddressed. The explored reaction mechanisms with possible intermediate/end products during discharge and charge are depicted in Fig. 2. The discharge reaction and the formation of intermediate/end products do not follow a precisely reversible path during the charge reaction and the formation of products.

Jaekook Kim is a Professor at the Department of Materials Science and Engineering, Chonnam National University (CNU), South Korea since 2003. He completed his B.S. and M. S. (1991) in Inorganic Materials Engineering at CNU. He obtained his Ph.D from the University of Texas, Austin. He worked as a staff scientist at Argonne National Laboratory, USA for 4 years. He has more than 300 international journal papers and several domestic and international patents to his credit and his research focuses on design and development of electrode materials for Li/Na and Zn batteries energy applications.
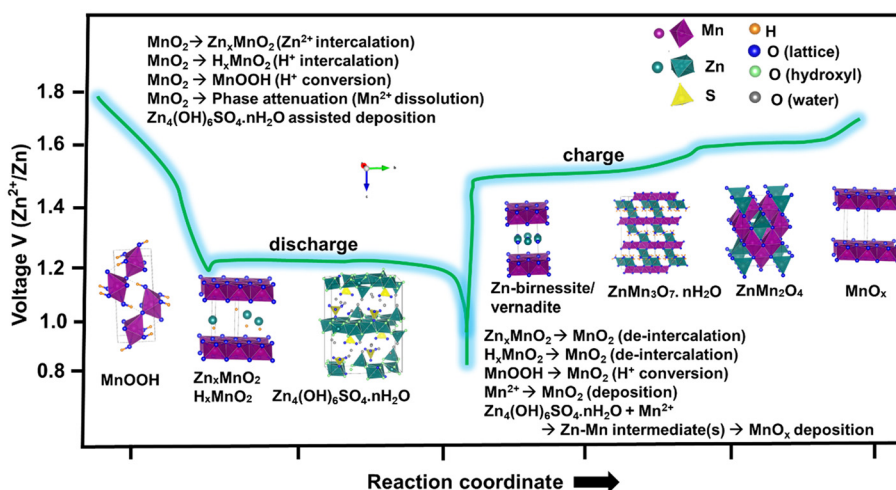
Jaekook Kim

A crucial study on the absence of Mn^{2+} additives in the ZnSO$_4$ electrolyte suggested that the choice of MnO$_2$ polymorphs is insignificant as the achieved capacities and charge–discharge curve profiles of different polymorphs remained almost identical after a few tens of cycles, while their initial discharge profiles varied.[10] This might result from common phase transformation in the structure of MnO$_2$ during cycling. In such a case, electrolyte pH regulation becomes critical. However, the initial variation in discharge profiles resulting from diversity in the crystal structures of these polymorphs requires an in-depth analysis. From detailed experimental studies along with *in situ* electrochemical quartz crystal microbalance (EQCM) analysis on the Zn–MnO$_2$ and Zn–Csp (super P carbon) electrodes containing aqueous 2 M ZnSO$_4$ + 0.2 M MnSO$_4$ electrolytes, it was observed that the formation of ZHS is from an intermediate amphoteric complex of (Zn(H$_2$O)$_x$(OH)$_2$), generally represented as Zn(OH)$_2$. This complex results from the deprotonation of the solvated [Zn(H$_2$O)$_6$]$^{2+}$ complex in the electrolyte which acts as a weak Brønsted acid. This confirms that the MnO$_2$–Mn^{2+} electrodeposition–dissolution reaction follows H$^+$ insertion into MnO$_2$ and not through intercalation.[11] Notably, irrespective of the type of positive cathode, with or without MnO$_2$, the study found that the electrochemical features are fingerprinted once the few initial cycles are completed. We also observed that the electrochemical charge–discharge curves are identical, irrespective of the type of polymorph of MnO$_2$, crossing few initial charge–discharge cycles, confirming that ZHS phase nucleation begins at ~1.3 V due to the presence of hydroxide ions resulting from the participation of protons in the MnO$_2$ and Mn dissolution. This slows down the pH variation below 1.3 V and the phase intensifies continuously until the discharge end. During charging, around 1.5 V, the ZHS phase starts dissolving reversibly (it can react with Mn^{2+} ions remaining in the electrolyte), and Mn^{2+}–MnO$_2$ deposition occurs as the charging progresses. The pH variation in the initial and subsequent cycles is quite com-

Fig. 2 Despite showing many similarities in their electrochemical charge–discharge curves, different polymorphs of MnO_2 with or without Mn^{2+} additives in the $ZnSO_4$ electrolyte have been proposed to have diverse mechanisms in the literature. These mechanisms with the respective intermediate/end products have been analyzed through plausible operando and non-operando techniques.

plicated to understand. Different pH variation trends within region I and region II within the first cycle have been reported.[12,13] This results in the nature of polymorphs, type of electrolyte with and without Mn^{2+} additives, aging time, and their initial pH values that can strongly affect the pH variation and resulting reaction during the electrochemical reaction.

Considering the above discussion, the present commentary article revives the call for this implicit controversial issue to converge towards an explicit mechanism that can be widely accepted. To achieve this anticipated goal, we provide a roadmap that recommends three critical strategies to be implemented as follows.

3. Roadmap strategies

(i) Operando experiments on selected crystalline MnO_2 polymorphs to lead the way in shedding more light on the reaction mechanism.

Specifically, we propose δ-MnO_2 ($R\bar{3}m$) with a layered (2D) structure (interlayer spacing $d \approx 7$ Å), α-MnO_2 with 2×2 and 1×1 tunnel type (1D), β-MnO_2 with 1×1 tunnel type (1D), and γ-MnO_2 with 1×2 and 1×1 tunnel type (1D) as optimal choices for observing real-time ion storage (intercalation-based redox reactions) due to varied first cycle electrochemical charge–discharge traces. Among them, layered δ-MnO_2, as evidenced by its lattice plane, shifts during the second discharge/ charge reaction by operando analysis,[14] which is helpful in understanding the intercalation mechanism, but still it is difficult to identify the type of intercalated ion and phase.[15] Other MnO_2 polymorphs have failed to reveal the intercalation phenomenon due to their distinct structures, making them incapable of elucidating the mechanism through operando XRD. It is advisable to rely on robust operando techniques to eliminate errors caused by unintentional blunders during

sample handling and misinterpretation of the subsequent analysis in Zn–MnO_2 batteries, which could cause delays in understanding the underlying mechanism. Recent concerns about conflict of interest regarding the proposed electrochemical reactions in Zn–Mn aqueous batteries have been addressed with supportive evidence from electrolyte pH and the implementation of adapted charging protocols.[16,17] Reliable operando XRD analyses have aligned with the absence of intermediate or end products of MnOOH during discharge,[9] neglecting a possible H^+ conversion reaction that was previously proposed as an essential electrochemical mechanism through non-operando analyses.[18] However, some reports argue that due to the amorphous characteristic of MnOOH, its confirmation through operando XRD analysis remains inconclusive and should be considered when addressing related mechanisms.

Significantly, irrespective of the suggested polymorphs and the nature of inserted ions, interconnected MnO_2 (Mn^{4+}–Mn^{2+} electrodeposition–dissolution) is observed through peak attenuation in operando XRD analysis, confirming its contribution arbitrarily.[7] Operando extended X-ray absorption fine structure analysis (X-ray absorption spectroscopy, XAS)[8] confirms multi-step Zn–Mn complex deposition–dissolution or deposition–conversion, as irreversible phases formed during the charge reaction, affirming its contribution to the reaction mechanism. This Zn–Mn multi-step reaction was proposed to be identical and independent of the polymorphs.[19] Therefore, real-time analyses, including all polymorphs, particularly tunnel and layered MnO_2, should be conducted under similar reaction conditions with known electrolyte pH to reveal these multi-step reactions. Utilizing operando XAS analysis, alongside electron paramagnetic resonance (EPR) without an Mn^{2+} additive in the electrolyte allows for cathode and electrolyte examinations, distinguishing Mn^{4+}, Mn^{3+}, and Mn^{2+} ions and thereby ease in understanding the electrochemical mecha-

nism. This cathode study can identify potential $Mn^{4+} \Leftrightarrow Mn^{3+/2+}$ conversions, offering a well-resolved hyperfine structure from diluted Mn^{2+} ions (electrodissolution to the electrolyte), impacting the MnO_2 EPR signal distinctly. It can also aid in understanding the Mn^{4+} and Mn^{3+} intermediate and addresses the Zn–Mn multi-step reaction at the cathode during charge, considering altered Mn^{4+} dipole–dipole and exchange interactions (Mn^{4+}–O^{2-}–Mn^{4+} and Mn^{4+}–O^{2-}–Mn^{3+} sites in MnO_2) with peak broadening. This study also aids in understanding the number of electrons transferred during MnO_2 conversion.

(ii) Differentiating the magnitude of intercalation and electrodissolution reactions of selected MnO_2 polymorphs in tuned electrolytes with the pH varying between 4 and 5.

A pool of electrolytes with the pH varying between 4 and 5, resulting in varying H^+ concentrations, can ultimately help in differentiating related reaction mechanisms for different polymorphs of MnO_2. This action can be helpful to distinguish the degree of H^+ intercalation and the Mn^{2+} depth of electrodissolution, both of which are strongly dependent on the electrolyte pH, during the electrochemical reaction. By directly comparing the results from using electrolytes with varying pH values, one can possibly differentiate the reaction mechanism as a function of H^+. In a recent study, by varying the electrolyte pH within the range of 4.0–5.3, the galvanostatic discharge response tends to display a pH-dependent first discharge profile with altered solid-solution and plateau-type profiles.[10] However, after a few cycles, the discharge trace tends to become identical, inferring a common electrochemical mechanism. Therefore, more research on this direction would be recommended.

(iii) Distinguishing the intercalating carrier ions through electrolyte isotope labelling.

Subsequently, a comprehensive analysis utilizing reliable operando techniques in conjunction with XRD analysis will determine the intercalation feasibility for driving the electrochemical mechanism. This assessment aims to ascertain, irrespective of any MnO_2/Mn^{2+} electrodeposition–dissolution contribution, whether the driving force is exclusively Zn^{2+} or H^+ or collectively Zn^{2+} and H^+ ions? The proposed facile approach involves employing isotope labeling in the electrolyte (either in Zn^{2+} salts or water solvent) to trace the source of intercalation (Fig. 3).

For instance, a non-radioactive Zn^{2+} salt, such as $^{70}ZnSO_4 \cdot xH_2O$, can be an electrolyte agent to monitor intercalation phenomena in the MnO_2 lattice. This approach aids in analyzing potential ^{70}Zn–O binding effects through operando neutron-based techniques, including neutron powder diffraction, neutron imaging, and neutron depth profiling. The neutron scattering power varies for different isotopic substitutions, enhancing sensitivity to locate positions. Supplementary analyses, such as solid-state ^{70}Zn-NMR, EQCM, operando-pH, and X-ray CT (refinement), further support these findings.[20]

Furthermore, a reported study suggested that the galvanostatic first discharge–charge voltage traces of electrochemically manganese dioxide and chemically manganese dioxide γ-MnO_2 polymorphs are comparable with subsequent cycles, indicating H^+ insertion into MnO_2 rather than intercalation.[11] We suggest that these candidates are optimal for understanding the electrochemical mechanism of Zn–MnO_2 batteries for further development.

Manganese electrodeposition–dissolution: a key electrochemical reaction in a broad potential window

Since the Mn-electrodissolution/deposition reaction involves protons in an acidic environment, its electrodissolution/deposition potential can vary depending on the pH of the electrolyte.[21] However, its working potential is much lower than 1.23 V *vs.* SHE for the following half-cell reaction: $MnO_2 + 4H^+ + 2e^- \leftrightarrow Mn^{2+} + 2H_2O$ under standard conditions of pH = 0 and $[a_{Mn^{2+}}] = 1$. In a full cell with a paired Zn anode, the expected electrodissolution/deposition potential would be predicted to be lower than ~1.9 V *vs.* Zn^{2+}/Zn, due to non-standard electrochemical conditions, with the electrolyte pH around 4.2. Similarly, in a mildly acidic aqueous electrolyte containing Zn salt, the availability of both H^+ and Zn^{2+} ions is prominent. However, their intercalation mechanism into the MnO_2
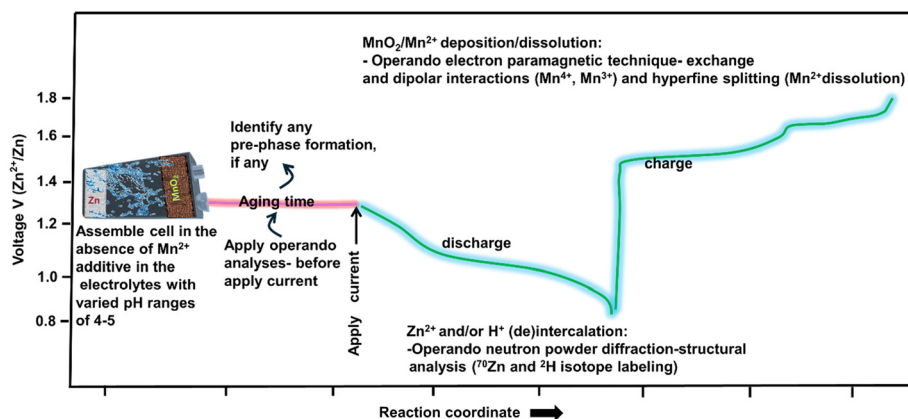

Fig. 3 Plausible forecast road map to distinguish Zn^{2+} *vs.* H^+ intercalation from MnO_2/Mn^{2+} electrodeposition–dissolution in layered MnO_2 through isotope labeling, operando neutron and electron paramagnetic resonance analyses.

cathode is yet to be proven through standard analyses as different schools of thought remain intact.[9,11,15] Based on the Nernst equation and available experimental results on α-MnO$_2$, the calculated electrodissolution potential during discharge is varied from approximately 1.6 to 1.3 V, where the initial/final pH and dissolved [Mn^{2+}] of the electrolyte are found to be 4.2/5.5 and 20/200 ppm, respectively (concentration has been converted into molarity as it is difficult to calculate the activity of dissolute Mn^{2+} in the electrolyte and hence the predicted potential region is not precise, but valued). This prediction reveals that pH variation is dominant until the voltage reaches 1.3 V. Below this threshold, due to the domination of the ZHS phase, pH variation is controlled.

Notably, the process of manganese dissolution could be initiated before applying current in the electrochemical cell, i.e., at an open circuit. With this insight, we conducted ab initio molecular dynamics (AIMD) simulations to investigate the potential dissolution of Mn atoms from surface active materials into a ZnSO$_4$ aqueous electrolyte. AIMD simulations are a well-established tool for exploring atomic-scale interactions and dynamics in condensed matter systems, particularly for studying the early stages of surface reactions and dissolution phenomena. In our work, AIMD was employed to probe the initial interactions between Mn-containing electrode surfaces and the ZnSO$_4$/H$_2$O electrolyte. We modelled three discharged electrode surface phases—Zn-intercalated ZnMn$_2$O$_4$, proton-converted MnOOH, and low-valence MnO—in the presence of Zn, SO$_4$, and H$_2$O molecules. These systems were designed to represent possible surface compositions during deep discharge. Through AIMD simulations, we monitored the evolution of atomic positions and analysed the displacement behaviour of Mn atoms as a proxy for their dissolution tendencies. Our results reveal distinct displacement trends for Mn atoms across different surface chemistries, providing molecular-level insights into the stability and interaction of each system with the electrolyte. The initial and final configurations of the simulation cells are presented for easy identification (Fig. 4). By analyzing the dynamics and displacement behavior of Mn atoms, distinct trends emerge, providing insight into the dissolution tendencies and chemical interactions of each system. In ZnMn$_2$O$_4$, the observed Mn displacements predominantly show inward movement in the z-direction, with minimal lateral adjustments (Fig. 4a). This suggests that the Mn atoms are stabilized either closer to the surface or within the crystal lattice, likely influenced by the presence of Zn and SO$_4$ ions. The relatively stable or inward movement of Mn atoms in the z-direction might indicate a system that is less prone to dissolution under these conditions, with longer simulation times potentially needed to observe significant Mn ion leaching.[22–24]

In the MnOOH system, shown in Fig. 4b, the displacement behavior presents a more complex scenario. Most Mn atoms exhibit inward movement toward the surface, consistent with stabilization or surface relaxation. However, a subset of Mn atoms shows outward displacements. This is a strong indicator of these atoms moving outward into the surrounding space, signaling their detachment from the surface. The Mn disproportionation reaction of 2Mn^{3+} into Mn^{4+} and Mn^{2+} may play a key role in promoting these outward shifts, as it facilitates detachment of Mn atoms from their lattice sites.[22] Compared to ZnMn$_2$O$_4$, MnOOH appears more prone to dissolution. MnO, on the other hand, shows the strongest evidence of dissolution among the three systems. Significant outward z-displacements of Mn atoms point to the detachment of Mn from the surface and potential formation of Mn^{2+} ions in solution, as depicted in Fig. 4c. The pronounced lateral displacements in MnO further highlight enhanced surface dynamics driven by interactions with Zn and SO$_4$ ions. The presence of H$_2$O in the system likely facilitates solvation and transport of Mn^{2+} ions, enhancing the dissolution process. These results indicate that MnO is the most dissolution-prone system under the given conditions, reflecting its chemical and structural susceptibility to ion leaching. The dissolution tendencies of Mn atoms vary significantly across the three systems influenced by their intrinsic structural properties and interactions with Zn, SO$_4$, and H$_2$O molecules. These simulation results provide valuable insights into the dissolution mechanisms of Mn-based materials in ZnSO$_4$ electrolytes.
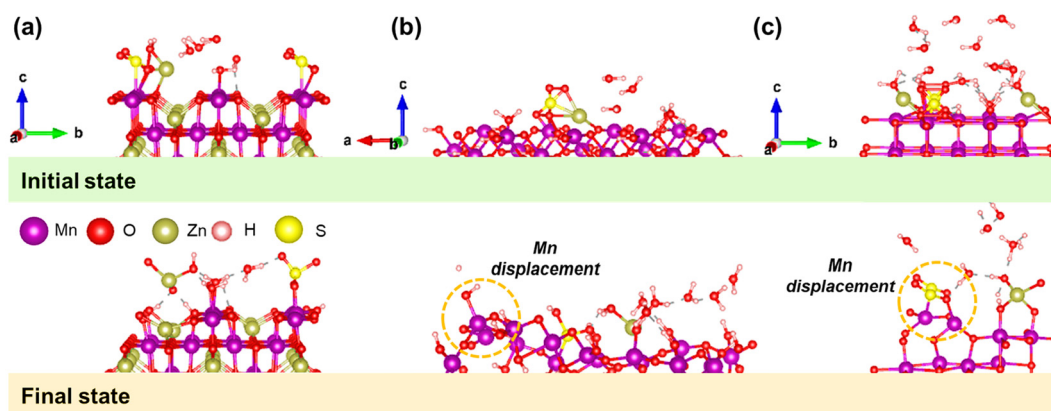

Fig. 4 Initial and ab initio molecular dynamic simulated final states of (a) ZnMn$_2$O$_4$, (b) MnOOH, and (c) MnO surface slabs.

4. Conclusive remarks

Critical questions surrounding the electrochemical mechanism of aqueous Zn-ion batteries must be addressed promptly through essential electrochemical studies using operando techniques with in-depth non-operando/computational support. Using selected polymorphs of MnO_2 to monitor structural evolution for the initial cycle and after a few cycles as a reference to address skeptical intercalation issues carefully is highly recommended in combination with operando neutron and electron paramagnetic analyses in different $ZnSO_4$ electrolytes with subtle pH variations, within the limit of 4–5, supported by other relevant methods including operando XAS. Most research studies support electrodeposition–dissolution as a major reaction contribution, regardless of the type of polymorphs, leaving the ion intercalation reaction to be verified in all polymorphs of MnO_2, except the layered one, whose confirmation has already been witnessed, without knowing the type of intercalating ion. Thus, it is imperative to develop more novel concepts and techniques that effectively support the primary electrochemical mechanism of Zn–MnO_2 AZIBs, given their ongoing progression. Despite a few commercial challenges, a few recent academic publications and a few startups in the Zn–MnO_2 batteries have successfully garnered increased public attention.

Data availability

The simulation data that support the findings of this study are available at https://github.com/hilmyalfaruq/vaspsimulation.

Conflicts of interest

The authors have declared that there are no competing interests.

Acknowledgements

References

1 D. Chao, W. Zhou, F. Xie, C. Ye, H. Li, M. Jaroniec and S.-Z. Qiao, *Sci. Adv.*, 2020, **6**, eaba4098.

2 S. W. D. Gourley, R. Brown, B. D. Adams and D. Higgins, *Joule*, 2023, **7**, 1415–1436.

3 G. Li, L. Sun, S. Zhang, C. Zhang, H. Jin, K. Davey, G. Liang, S. Liu, J. Mao and Z. Guo, *Adv. Funct. Mater.*, 2024, **34**, 2301291.

4 Y. Zhang, Z. Chen, H. Qiu, W. Yang, Z. Zhao, J. Zhao and G. Cui, *NPG Asia Mater.*, 2020, **12**, 4.

5 https://www.enerpoly.com/technology#cell-pack.

6 https://salientenergyinc.com/.

7 B. Sambandam, V. Mathew, S. Kim, S. Lee, S. Kim, J. Y. Hwang, H. J. Fan and J. Kim, *Chem*, 2022, **8**, 924–946.

8 D. Wu, L. M. Housel, S. T. King, Z. R. Mansley, N. Sadique, Y. Zhu, L. Ma, S. N. Ehrlich, H. Zhong, E. S. Takeuchi, A. C. Marschilok, D. C. Bock, L. Wang and K. J. Takeuchi, *J. Am. Chem. Soc.*, 2022, **144**, 23405–23420.

9 Y. Yuan, R. Sharpe, K. He, C. Li, M. T. Saray, T. Liu, W. Yao, M. Cheng, H. Jin, S. Wang, K. Amine, R. Shahbazian-Yassar, M. S. Islam and J. Lu, *Nat. Sustain.*, 2022, **5**, 890–898.

10 U. Siamionau, Y. Aniskevich, A. Mazanik, O. Kokits, G. Ragoisha, J. H. Jo, S.-T. Myung and E. Streltsov, *J. Power Sources*, 2022, **523**, 231023.

11 I. Aguilar, P. Lemaire, N. Ayouni, E. Bendadesse, A. V. Morozov, O. Sel, V. Balland, B. Limoges, A. M. Abakumov, E. Raymundo-Piñero, A. Slodczyk, A. Canizarès, D. Larcher and J.-M. Tarascon, *Energy Storage Mater.*, 2022, **53**, 238–253.

12 C. F. Bischoff, O. S. Fitz, J. Burns, M. Bauer, H. Gentischer, K. P. Birke, H.-M. Henning and D. Biro, *J. Electrochem. Soc.*, 2020, **167**, 020545.

13 X. Xie, H. Fu, Y. Fang, B. Lu, J. Zhou and S. Liang, *Adv. Energy Mater.*, 2022, **12**, 2102393.

14 M. H. Alfaruqi, S. Islam, D. Y. Putro, V. Mathew, S. Kim, J. Jo, S. Kim, Y.-K. Sun, K. Kim and J. Kim, *Electrochim. Acta*, 2018, **276**, 1–11.

15 N. J. Herrmann, H. Euchner, A. Groß and B. Horstmann, *Adv. Energy Mater.*, 2024, **14**, 2302553.

16 H. Yang, T. Zhang, D. Chen, Y. Tan, W. Zhou, L. Li, W. Li, G. Li, W. Han, H. J. Fan and D. Chao, *Adv. Mater.*, 2023, **35**, 2300053.

17 H. Wang, T. Wang, G. Stevenson, M. Chamoun and R. W. Lindström, *Energy Storage Mater.*, 2023, **63**, 103008.

18 H. Pan, Y. Shao, P. Yan, Y. Cheng, K. S. Han, Z. Nie, C. Wang, J. Yang, X. Li, P. Bhattacharya, K. T. Mueller and J. Liu, *Nat. Energy*, 2016, **1**, 16039.

19 V. R. Kankanallu, X. Zheng, D. Leschev, N. Zmich, C. Clark, C.-H. Lin, H. Zhong, S. Ghose, A. M. Kiss, D. Nykypanchuk, E. Stavitski, E. S. Takeuchi, A. C. Marschilok, K. J. Takeuchi, J. Bai, M. Ge and Y.-C. K. Chen-Wiegart, *Energy Environ. Sci.*, 2023, **16**, 2464–2482.

20 Y. Zhang, Y. Liang, H. Dong, X. Wang and Y. Yao, *J. Electrochem. Soc.*, 2020, **167**, 070558.

21 D. Chao, W. Zhou, C. Ye, Q. Zhang, Y. Chen, L. Gu, K. Davey and S.-Z. Qiao, *Angew. Chem., Int. Ed.*, 2019, **58**, 7823–7828.

22 R. Benedek, *J. Phys. Chem. C*, 2017, **121**, 22049–22053.

23 K. Leung, *Chem. Mater.*, 2017, **29**, 2550–2562.

24 R. Benedek, M. M. Thackeray, J. Low and T. Bučko, *J. Phys. Chem. C*, 2012, **116**, 4050–4059.